Impact of fin spacing on temperature distribution in adsorption cooling system for vehicle A/C applications

*Amir Sharafian, Claire McCague, Majid Bahrami**

Laboratory for Alternative Energy Conversion (LAEC), School of Mechatronic Systems Engineering, Simon Fraser University, # 4300, 250-13450 102nd Avenue, Surrey, BC V3T 0A3, Canada

ARTICLE INFO

ABSTRACT

Effects of fin spacing on the temperature distribution in a finned tube adsorber bed are studied to decrease the temperature gradient inside the adsorber bed and minimize the adsorber bed to adsorbent mass ratio (AAMR) for vehicle air conditioning applications. Finned tube adsorber beds have shown higher specific cooling power and coefficient of performance, and low AAMR among the existing adsorber beds. A single-adsorber bed ACS with interchangeable heat exchangers is built and equipped with hermetic type T thermocouples. Two copper heat exchangers with 6.35 mm (1/4″) and 9.5 mm (3/8″) fin spacing are custom-built and packed with 2–4 mm silica gel beads. The experimental results show that by decreasing the fin spacing from 9.5 mm to 6.35 mm, the temperature difference between the fin and adsorbent reduces by 4.6 °C under the cycle time of 600 s and an adsorption to desorption time ratio (ADTR) of one. A greater reduction in the temperature gradient inside the adsorber bed with smaller fin spacing is observed for short cycle time operation, e.g. 600 s, compared to long cycle time operation, e.g. 1400 s. Finally, simultaneous comparison of the temperature gradient between the fins and AAMR against fin spacing indicates that the optimum fin spacing for a finned tube heat exchanger packed with 2–4 mm silica gel beads is about 6 mm.

Impact de l'espacement des ailettes sur la distribution des températures dans un système de froid à adsorption pour des applications de conditionnement d'air automobile

---

* Corresponding author. Tel.: +1 778 782 8538; fax: +1 778 782 7514.
  E-mail addresses: asharafi@sfu.ca (A. Sharafian), clairem@sfu.ca (C. McCague), mbahrami@sfu.ca (M. Bahrami).

Nomenclature

AAMR	adsorber bed to adsorbent mass ratio ($kg_{metal}\ kg^{-1}_{dry\ adsorbent}$)
ACS	adsorption cooling system
A/C	air conditioning
ADTR	adsorption to desorption time ratio
Ads.	adsorption
COP	coefficient of performance
Des.	desorption
FS	fin spacing

ICE	internal combustion engine
SCP	specific cooling power (W kg^{-1})
T	temperature (°C)

Subscript

ambient	ambient
bed	adsorber bed
cond	condenser
evap	evaporator

1. Introduction

Adsorption cooling systems (ACS) produce cooling power through utilization of low grade thermal energy, e.g. waste heat from an engine, and have received significant attention during the last decade mainly due to higher fuel prices, energy shortages, and stringent government environmental/emission regulations (Zhang and Wang, 1997; Lu et al., 2004; Verde et al., 2010). In a typical internal combustion engine (ICE), almost 70% of the total fuel energy is dissipated through the engine coolant and the exhaust gas in the form of waste heat (Farrington and Rugh, 2000). Also, auxiliary loads such as air conditioning (A/C) in light-duty vehicles increase the fuel consumption. The SFTP-SC03 driving cycle showed that a vapor compression refrigeration cycle (VCRC) in light-duty vehicles increases the fuel consumption by 28%, and CO_2 and NOx emissions by 71% and 81%, respectively (Hendricks, 2001). ACS is a promising alternative to VCRC for air conditioning that can reduce the fuel consumption and gas emissions, and increase the overall efficiency of vehicles. A working pair in ACS is a combination of an adsorbent (e.g., zeolite, silica gel, and activated carbon) and an adsorbate (e.g., water and methanol). These materials are environmentally friendly, non-toxic, non-corrosive, non-ozone depleting, and inexpensive (Demir et al., 2008).

A single-adsorber bed ACS consists of an adsorber bed packed with an adsorbent, and an adsorbate container. To produce cooling power, ACS cycle undergoes two main processes: heating-desorption-condensation and cooling-adsorption-evaporation. During the first process, the adsorber bed is heated up to desorb the adsorbate and pressure of the adsorber bed increases. Due to higher pressure of the adsorber bed than the adsorbate container, the vaporous adsorbate flows through the adsorbate container and is condensed inside the container. In the next process, the adsober bed is cooled down and the adsorbent adsorbs the adsorbate and pressure of the adsorber bed reduces. When pressure of the adsober bed drops below the adsorbate container, liquid adsorbate inside the adsorbate container is evaporated due to the suction of the adsorber bed and cooling effect happens inside the adsorbate container. Following these processes, the single-adsorber bed ACS produces evaporative cooling power intermittently. However, commercialization of ACS faces major challenges because of (i) low specific cooling power (SCP), which is defined as the ratio of the cooling load to the mass of dry adsorbent multiplied by the cycle time; and (ii) poor coefficient of performance (COP).
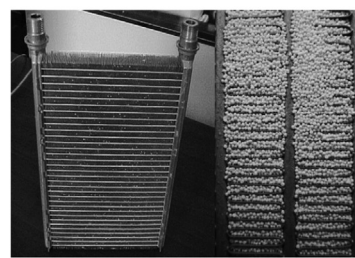
The low thermal conductivity of the adsorbent particles (~0.1–0.4 W m^{-1} K^{-1}) (Poyelle et al., 1999; Tamainot-Telto and Critoph, 2001; Freni et al., 2002) and low mass diffusivity of adsorbent–adsorbate pairs (~10^{-8} to 10^{-14} m^2 s^{-1}) (Sharafian and Bahrami, 2013) result in low heat and mass transfer rate inside the adsorber bed, and consequently, heavy and bulky ACS. Fins inside the adsorber bed decrease the heat transfer resistance caused by the adsorbent particles and increase the heat transfer surface area leading to improved adsorption and
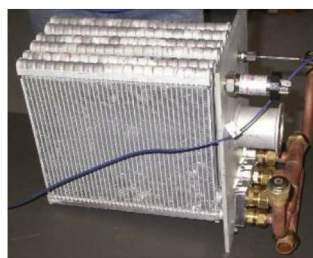
(a) Freni et al., 2007   (b) Verde et al., 2011   (c) Sapienza et al., 2011 and Aristov et al., 2012

Fig. 1 – **Finned** tube adsorber beds used in waste-heat driven ACS with high SCP and COP, and low AAMR (Sharafian and Bahrami, 2014).

Table 1 – Temperature measurements in the adsorbent packed bed.		
Ref. No.	Working pair	Purpose
Zhang and Wang (1999a, 1999b)	Zeolite 13X-water	Developing a non-equilibrium 3D model for heat and mass transfer in an adsorber bed
Eun et al. (2000a, 2000b)	Silica gel/expanded graphite-water	Measuring temperature in an adsorbent composite block and pure silica gel packed bed, and comparing their differences
Pentchev et al. (2002)	Zeolite 4A-water	Measuring the axial and radial temperature distributions inside the adsorbent packed bed under adiabatic, near adiabatic and non-adiabatic boundary conditions and developing a 2D numerical model
El-Sharkawy et al. (2006)	Activated carbon fiber-ethanol	Activated carbon fiber characterization and measuring its temperature variation during the adsorption process vs. time
Wu et al. (2009)	Zeolite 13X-water	Measuring the wall temperature of adsorbent packed bed to verify a numerical model
Zhao et al. (2012)	Activated carbon-methanol	Measuring temperature distribution in an adsorbent packed bed to verify a numerical model
Mahdavikhah and Niazmand (2013)	SWS 1L-water	Developing a numerical model to study the effects of fin height and spacing on the performance of ACS
White (2012)	Silica gel-water	Measuring temperature in a finned tube adsober bed to verify a numerical model

desorption processes for a shorter cycle time. However, adding fins increases the total mass of the adsorber bed which is not desirable especially for vehicle A/C applications that require light-weight systems. Recently, Sharafian and Bahrami (2014) critically reviewed the SCP, adsorber bed to adsorbent mass ratio (AAMR), and COP of more than 50 studies/experiments reported in the literature with a focus on adsorber beds to establish the state-of-the-art adsorber bed design. They categorized the available adsorber beds into nine types, namely, (1) spiral plate, (2) shell and tube, (3) hairpin, (4) annulus tube, (5) plate fin, (6) finned tube, (7) plate-tube, (8) simple tube, and (9) plate. Among the existing adsorber bed designs, finned tube adsorber beds are more desirable by showing higher SCP and COP, and lower AAMR. The common features of these adsorber beds, depicted in Fig. 1, are a large number of fins to increase the heat transfer surface area and small fin spacing to decrease the heat transfer resistance inside the adsorber bed. However, none of the reported adsorber beds in the literature were specifically designed for the ACS applications.

One way of establishing efficient heat transfer from a heat transfer fluid (HTF) to the adsorbent particles is to experimentally measure the temperature distribution inside the adsorber bed. In several studies and experiments, the temperature distribution inside packed beds of adsorbent particles has been measured (Zhang and Wang, 1999a, 1999b; Eun et al., 2000a; Eun et al., 2000b; Pentchev et al., 2002; El-Sharkawy et al., 2006; Wu et al., 2009; Zhao et al., 2012; Mahdavikhah and Niazmand, 2013; White, 2012). The highlights of these studies are summarized in Table 1.

As shown in Table 1, two main purposes of the temperature measurements in the adsorbent packed beds are to verify the accuracy of numerical models (Zhang and Wang, 1999a, 1999b; Pentchev et al., 2002; Wu et al., 2009; Zhao et al., 2012; Mahdavikhah and Niazmand, 2013; White, 2012) and compare loose grain adsorbent against the consolidated adsorbent (Eun et al., 2000a, 2000b). To our best knowledge, there is no experimental study available that shows the temperature distribution inside a finned tube adsorber bed to investigate the effectiveness of heat transferred to and from

the adsorbent particles and to establish optimum fin spacing. In this study, the effects of fin spacing on temperature distribution inside a finned tubed adsober bed and condenser/evaporator are investigated experimentally. The AAMR is one of the main factors in the ACS for vehicle applications. A lower AAMR means less 'dead' to 'live' mass ratio. As such, in the next step, the goal is to select a finned tube adsorber bed with proper fin spacing and acceptable AAMR through measuring the temperature inside the adsorber bed.

2. Experimental apparatus

ACS cycle works based on two main processes: heating-desorption-condensation and cooling-adsorption-evaporation. Following these steps, an ACS intermittently produces cooling power, such as data reported in Refs. (Boelman et al., 1995; Chua et al., 1999; Alam et al., 2000; Saha et al., 2009). In this study, a single-adsorber bed ACS was built to test different finned tube heat exchangers with different fin spacing. As shown in Fig. 2a, a vacuum chamber equipped with hermetic thermocouples was used as an adsorber bed
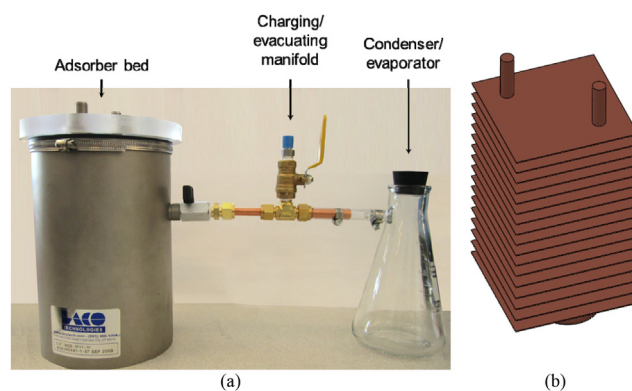
Fig. 2 – (a) Single-adsorber bed ACS experimental setup, and (b) schematic of finned tube heat exchanger located inside the adsorber bed.

and, a Buchner flask was used as a condenser/evaporator to visually monitor the condensation and evaporation processes. Silica gel beads with 2–4 mm diameters (3.2 mm average diameter) and water were selected as the working pair because the low regeneration temperature of silica gel (<95 °C) is similar to that of the engine coolant in ICE. This is ideal, especially when compared to activated carbon and zeolite with higher regeneration temperatures, 130 °C and 180 °C, respectively.

Two finned tube adsober beds with 6.35 mm (1/4″) and 9.5 mm (3/8″) fin spacing were built to study the effects of fin spacing on the temperature distribution inside the adsorber bed and condenser/evaporator under different cycle times and adsorption/desorption time ratios (ADTRs). The finned tube heat exchanger, shown in Fig. 2b, was made from copper plates and tubes and the fins were soldered to the tubes to minimize the thermal contact resistance between the heat exchanger parts. The finned section of the heat exchangers had 11.4–11.45 cm height to fit inside the adsorber bed.

Reducing the fin spacing can lead to an increase in the number of fins, heat transfer surface area and metal mass of the heat exchanger. It also decreases the amount of silica gel packed inside the heat exchanger, and, consequently, results in a higher AAMR. For instance, in the case where 2 mm silica gel beads are used, the minimum possible fin spacing for the heat exchanger would ideally be 2 mm. Our calculations showed that a finned tube heat exchanger with $9 \times 9 \times 0.0762$ cm (length × width × thickness) fins, 2 mm fin spacing and 11.4 cm finned section would have 42 fins, a total heat transfer surface area of 0.68 m^2 ($= 42 \times 0.09 \times 0.09 \times 2$) and a metal mass of 2307 g ($= 42 \times 9 \times 9 \times 0.0762 \times 8.9$ g cm^{-3}). This heat exchanger would hold only 531 g ($= 41 \times 9 \times 9 \times 0.2 \times 0.8$ g cm^{-3}) of silica gel. Thus, the AAMR becomes 4.34 ($= 2307$ g/531 g). To reduce this ratio, the only solution is to increase the fin spacing. The specifications of our two heat exchangers with 6.35 mm and 9.53 mm fin spacing as well as heating and cooling fluids inlet temperatures and mass

flow rates are summarized in Table 2. These fin spacing were selected such that the ratio of fin spacing to the average silica gel particles became approximately 2.0 (≈ 6.35 mm/3.2 mm) and 3.0 (≈ 9.53 mm/3.2 mm), respectively.

As shown in Table 2, the heat exchanger with 6.35 mm fin spacing packed with 770 g of silica gel provides an AAMR of 1.27, whereas that of with 9.5 mm fin spacing packed with 820 g of silica gel gives an AAMR of 0.87, respectively.

Fig. 3 shows the location of nine hermetic thermocouples mounted inside the heat exchangers with 6.35 mm and 9.5 mm fin spacing to monitor the temperature distribution during the adsorption and desorption processes. The hermetic thermocouples used inside the adsorber bed were type T with accuracy of ±1.0 °C supplied by PAVE Technology Company. In Fig. 3, thermocouples TC0 and TC8 measure the working fluid inlet and outlet temperatures to the adsorber bed. Thermocouples TC1 and TC2 measure the temperatures on the fin wall and at the center of the first two fins, respectively. Thermocouples TC3 and TC5 also display the temperatures at the center of the fins whereas thermocouples TC4, TC6 and TC7 show the temperatures at the corners of the fins. To measure the condenser/evaporator and ambient temperatures, type T thermocouples with accuracy of ±1.0 °C supplied by Omega were used. A LabVIEW interface was developed to monitor and record the temperatures as a function of time.

3. Results and discussion

Fig. 4 shows the temperature distribution and pressure profile in the adsorber bed with 9.5 mm fin spacing and temperature variation in the condenser/evaporator under the cycle time of 1400 s and ADTR of one. It can be seen in Fig. 4 that after the first cycle (time > 1400 s), temperature and pressure profiles in the adsorber bed are replicated. Fig. 4a demonstrates that as the ambient temperature is lower than water vapor temperature during the desorption process, the flask behaves as a condenser and condensation occurs on the walls of the flask. During the adsorption process, the flask serves as an evaporator. When the adsorber bed is cooled down, the pressure inside the adsorber bed reduces, and consequently, the liquid water inside the flask starts evaporating. As a result of evaporation, the liquid water temperature drops and cooling occurs. The adsorption and desorption processes with an ADTR of one (700 s adsorption, 700 s desorption) are demarcated in Fig. 4.

To assure the reproducibility of the measured experimental data, the evaporator temperature was measured on two different days. Fig. 5 shows the temperature of evaporator at the end of adsorption process when it is connected to the adsorber bed with 9.5 mm fin spacing under different cycle times and ADTR of one. It can be seen in Fig. 5 that the measured data on different days under the same operating conditions are the same. Both have a maximum relative difference of 5%; thus it can be concluded that the results are reproducible. Also, Fig. 5 indicates that the evaporator temperature reduces by increasing the cycle time. Longer cycle time permits a greater heat removal from the adsorbent particles, a greater adsorbate uptake by the adsorbent particles and, consequently, reaching to lower evaporation

Table 2 – Specifications of heat exchangers and heat transfer fluids.

| Parameters	Heat exchanger	
	6.35 mm fin spacing	9.53 mm fin spacing
No. of fins	17	12
Mass of heat exchanger	978 g	716 g
Mass of silica gel	770 g	820 g
AAMR	1.27 (978 g/770 g)	0.87 (716 g/820 g)
Heat transfer surface area	0.266 m^2	0.188 m^2
Mass of water in the condenser/ evaporator	80 g	
Heating water flow rate to the bed	0.062 kg s^{-1} (3.72 L min^{-1})	
Heating water inlet temperature to the bed	88–93 °C	
Cooling water flow rate to the bed	0.03 kg s^{-1} (1.78 L min^{-1})	
Cooling water inlet temperature to the bed	28–33 °C	
Fin thickness	0.0762 cm (0.03″)	
Fin dimensions	9 × 9 cm	
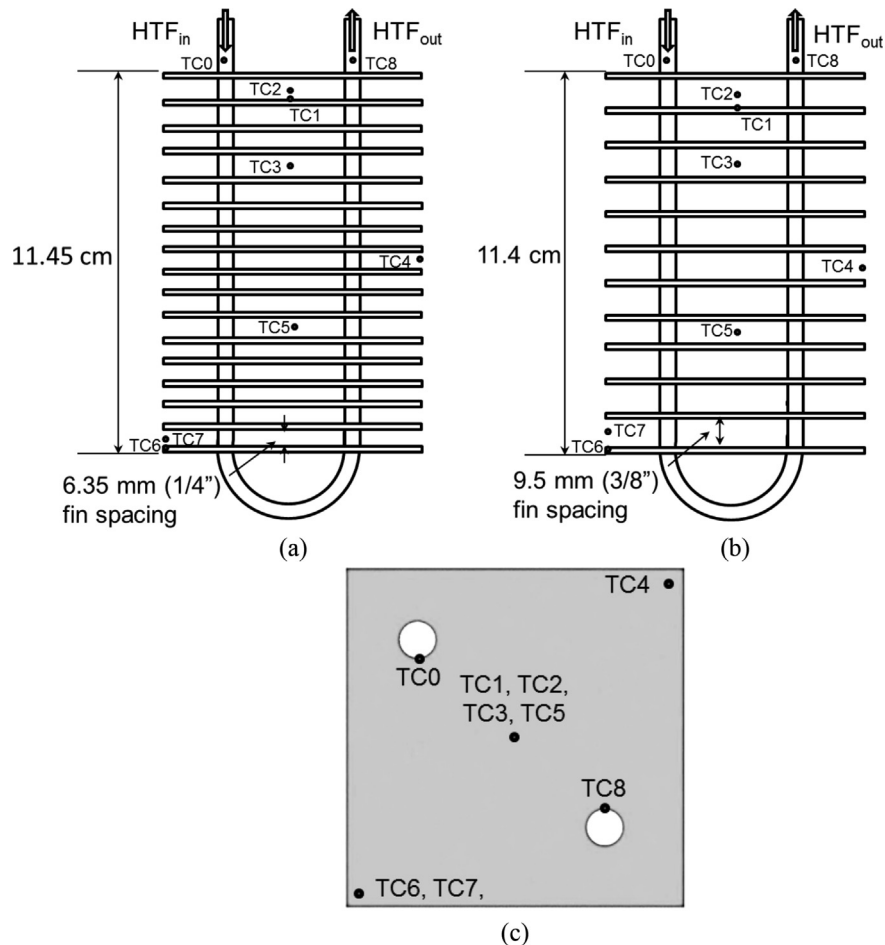
Fig. 3 − **Location of thermocouples inside the heat exchanger with (a) 6.35 mm fin spacing and (b) 9.5 mm fin spacing, and (C) top view.**

temperature. However, the cycle time also depends on and is limited by the vehicle driving cycle. For example, the total daily commute time in the U.S. is about 40 min, ≈20 min to work and ≈20 min returning home (Lambert and Jones, 2006a, 2006b). To accelerate heat and mass transfer to and from the adsorbent particles, the adsorber bed fin spacing should be reduced to minimize the thermal resistance of adsorbent particles.

Fig. 6 shows the temperature differences between thermocouples TC1 and TC2 at the end of adsorption and desorption processes under different cycle times and ADTRs. Fig. 6 shows that by increasing the cycle time from 600 s to 1400 s, the temperature gradient between TC1 and TC2 gradually reduces as a result of more heat transfer to and from the adsorbent particles. However, Fig. 6 indicates that the temperature differences between TC1 and TC2 in the heat exchanger with 6.35 mm fin spacing are much lower than those in the heat exchanger with 9.53 mm fin spacing, specifically under short cycle times. For example, under the cycle time of 600 s and ADTR of one, Fig. 6a, the temperature differences between TC1 and TC2 at the end of desorption process are 3.1 °C and 7.7 °C for the heat exchangers with 6.35 mm and 9.53 mm fin spacing, respectively.

Fig. 6a indicates that the temperature differences between TC1 and TC2 at the end of desorption process and ADTR of one are always higher than those at the end of the adsorption process. Adsorption is an exothermic process and, therefore, heat generation occurs throughout the adsorber bed and the temperature difference between the adsorbent particles reduces. Whereas desorption is an endothermic process and adsorbent particles gain heat from an internal heat source during which the temperature difference between the adsorbent particles increases. As a result, it can be concluded that the largest temperature gradient inside the adsorber bed, under ADTR of one, happens during the desorption process.

Figs. 6b and c show that by increasing the ADTR from one to three, the temperature difference between TC1 and TC2 does not vary significantly at the end of adsorption process for both heat exchangers. However, the temperature difference between TC1 and TC2 at the end of desorption process increases for the heat exchanger with 9.35 mm fin spacing. For instance, the temperature difference between TC1 and TC2 at the end of desorption process and cycle time of 600 s increases from 7.7 °C to 10.9 °C in the heat exchanger with 9.35 mm fin spacing by increasing the ADTR from one to three, respectively.
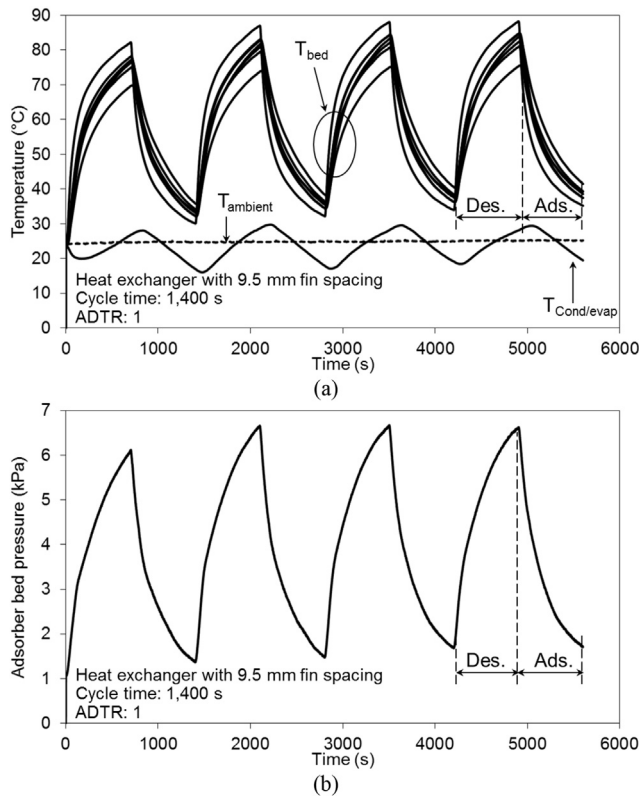
Fig. 4 – (a) Temperature distribution and (b) pressure profile in the single-adsorber bed ACS under the cycle time of 1400 s and ADTR of one.

Fig. 7 shows the temperature differences between TC6 and TC7 at the end of adsorption and desorption processes in the adsorber beds with 6.35 mm and 9.5 mm fin spacing under different cycle times and ADTRs. The location of thermocouples TC6 and TC7 are different from thermocouples TC1 and TC2. Thermocouples TC6 and TC7 are located at the corner of the fins and are in contact with the adsorbate flow which has different temperature than the adsorbent particles. As opposed to thermocouples TC1 and TC2 that are located at the center of the fins and are exposed to the vaporous adsorbate flow with the same temperature as the adsorbent particles. As
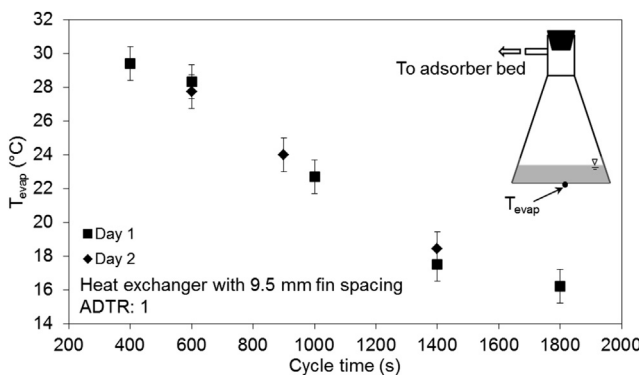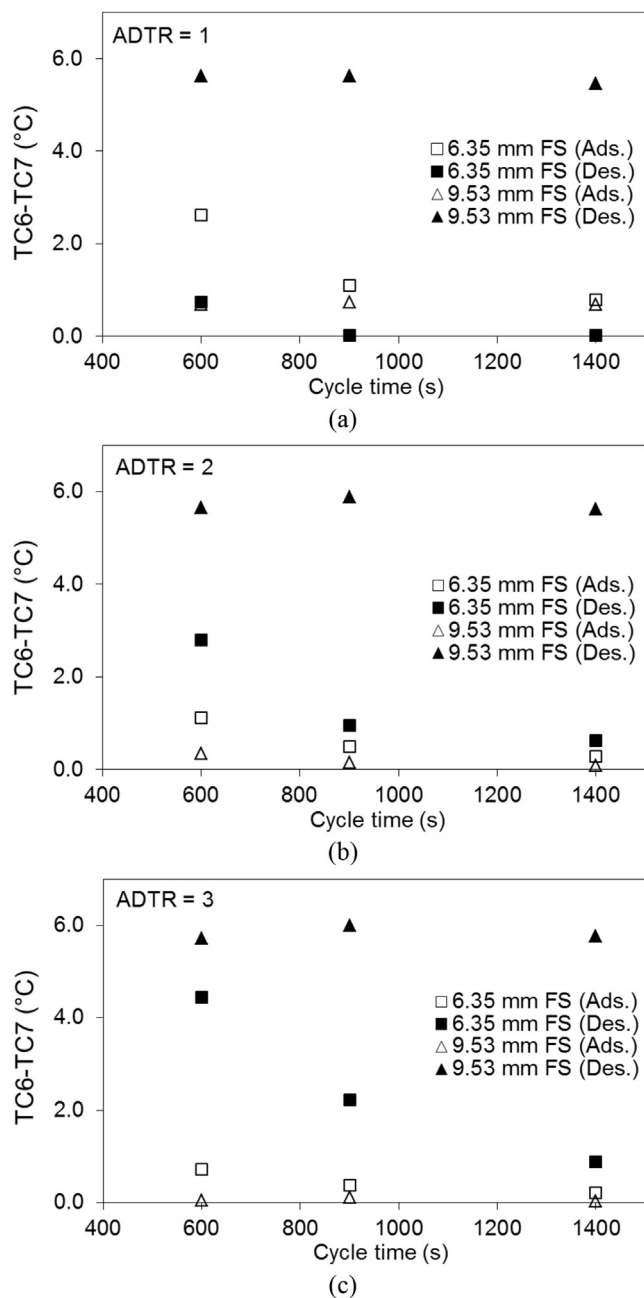

Fig. 5 – Evaporator temperature at the end of adsorption process vs. cycle time.
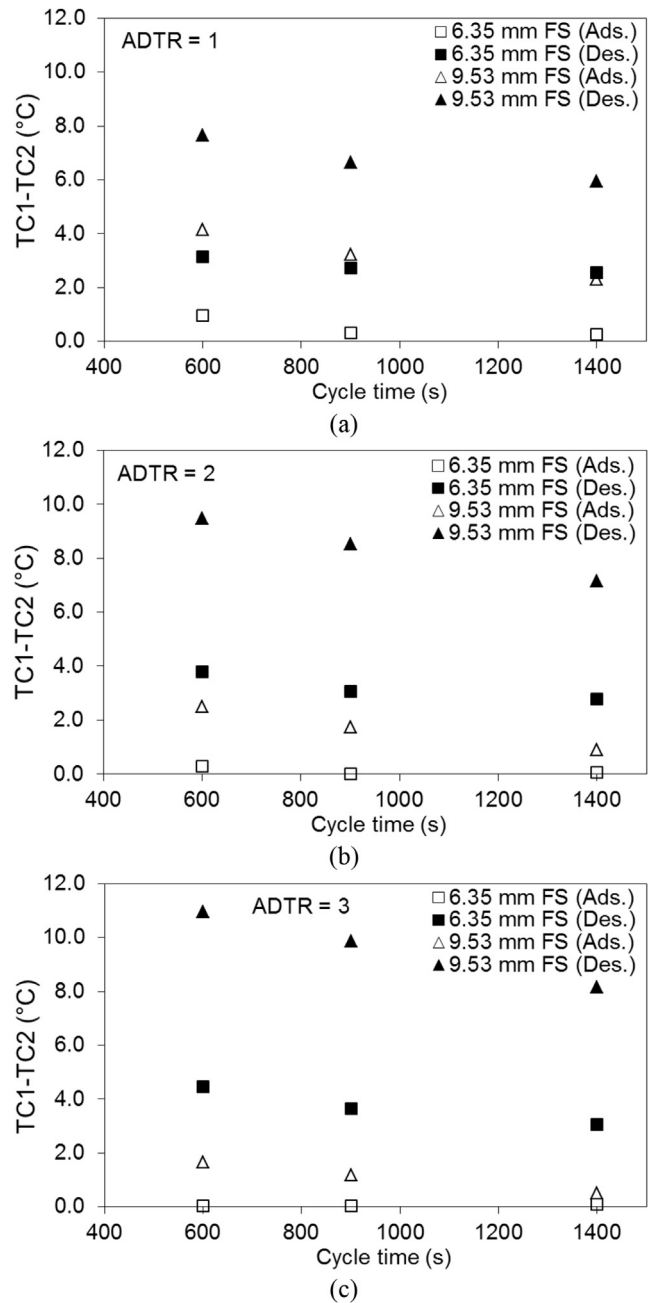
Fig. 6 – Temperature differences between thermocouples TC1 and TC2 at the end of adsorption and desorption processes for adsorber beds with 6.35 mm and 9.5 mm fin spacing under different cycle times and ADTRs.
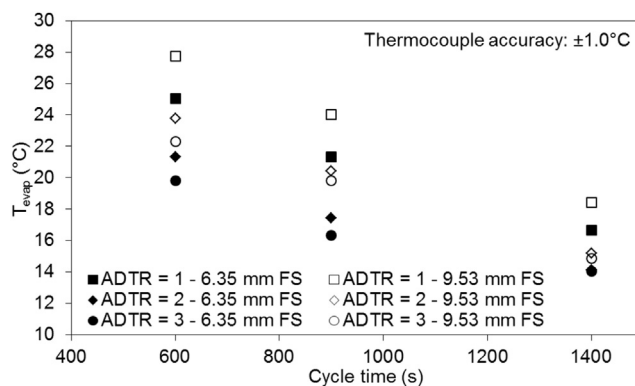
a result, the temperatures measured by TC6 and TC7 are not merely caused by heating and cooling of the adsorbent particles. For example, during the adsorption process, TC6 and TC7 measure the adsorbent particles temperature and the cold vaporous adsorbate which comes from the evaporator. As such, it can be seen in Fig. 7 that in the heat exchanger with 9.53 mm fin spacing, temperature differences between TC6 and TC7 do not change significantly by increasing the cycle time from 600 s to 1400 s. However, by reducing the fin spacing from 9.53 mm to 6.35 mm, the temperature difference

Fig. 7 – Temperature differences between thermocouples TC6 and TC7 at the end of adsorption and desorption processes for adsorber beds with 6.35 mm and 9.5 mm fin spacing under different cycle times and ADTRs.

Fig. 8 – Effects of fin spacing on the evaporator temperature under different cycle times and ADTRs.

processes. The adsorbent particles at the center of the fins are only heated up and cooled down by the fins and are affected by their adjacent adsorbent particles. However, the adsorbent particles at the edge of the fins are mainly influenced by the adsorbate temperature unless otherwise fin spacing becomes small.

The effects of fin spacing on the temperature of evaporator at the end of adsorption process are shown in Fig. 8. It can be seen in Fig. 8 that the heat exchanger with 6.35 mm fin spacing produces lower evaporation temperatures than that with 9.53 mm fin spacing, especially at the cycle time of 600 s. Also, Fig. 8 demonstrates that the evaporator temperature highly depends on the ADTR. In A/C systems, the evaporator pressure is lower than the condenser pressure. The low evaporation pressure in ACS results in a slower uptake rate of adsorbate by the adsorbent particles, thus, the adsorption time should be increased to charge the adsorber bed. Fig. 8 depicts the two practical solutions to increase the adsorption uptake of adsorbate by the adsorbent particles. The first solution is to increase ADTR from one to three. However, in order to reach an ADTR of three, four adsorber beds are required (i.e., one adsorber bed desorbs and three adsorber beds adsorb the adsorbate). A four-adsorber bed ACS leads to a heavy and bulky system; which is not practical for vehicle applications. The second solution is to increase the cycle time.

Fig. 9 – Temperature difference between thermocouples TC1 and TC2 at the end of desorption process under different cycle times and AAMR vs. adsorber beds with different fin spacing.

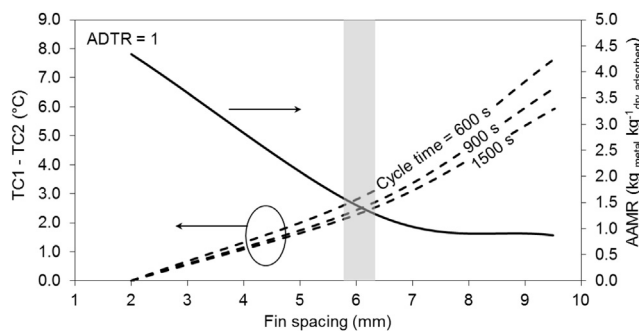between TC6 and TC7 changes under different cycle times and ADTRs.

To magnify the effects of fins in heat transfer, Fig. 7 shows that fin spacing needs to be reduced. The heat exchanger with 6.35 mm fin spacing results in reducing the temperature differences between TC6 and TC7, specifically at the end of the desorption process. By comparing Figs. 6 and 7, it can be shown that the adsorbent particles experience different temperatures during the adsorption and desorption

As shown in Fig. 8, the difference between the evaporator temperatures at cycle time of 1400 s is not noticeably affected by ADTR. In the case of using the heat exchanger with 6.35 mm fin spacing under cycle time of 1400 s, the maximum evaporation temperature difference between ADTR of one and three is equal to 2.6 °C.

Based on the measured temperatures inside the single-adsorber bed ACS, one can conclude that to have an adsorber bed with a more uniform temperature distribution between the adsorbent particles and an ACS with smaller foot-print and weight, the fin spacing must be reduced and ADTR should be kept at one. To find the optimum fin spacing based on the experimental data, the temperature differences between thermocouples TC1 and TC2 at the end of desorption process and AAMR are plotted against adsorber beds with different fin spacing in Fig. 9. As mentioned in Section 2, our calculations showed that the AAMR for the heat exchanger with 2 mm fin spacing would be equal to 4.34 and the temperature difference between thermocouples TC1 and TC2 is negligible (~0). The other data to generate Fig. 9 are provided in Table 2 and Fig. 6a.

Fig. 9 shows that by increasing the fin spacing from 2 mm to 9.5 mm, the temperature difference between thermocouples TC1 and TC2 increases from zero to 7.7 °C under the cycle time of 600 s whereas AAMR reduces from 4.34 to 0.87. For vehicle applications, the AAMR should be minimized; however, it should not significantly affect the performance of the ACS. To this end, the intersection of the temperature difference between thermocouples TC1 and TC2 under different cycle times, and AAMR is selected as the optimum fin spacing. The gray region in Fig. 9 demarcates the optimum fin spacing (about 6 mm) for a finned tube adsorber bed packed with 2–4 mm silica gel beads.

4. Conclusion

Effects of fin spacing on the temperature distribution in a finned tube adsorber bed were studied experimentally. Two heat exchangers with 6.35 mm and 9.5 mm fin spacing were custom-built and packed with 2–4 mm silica gel beads. The results showed that the adsorbent particles experience different temperatures at different locations of the adsober bed. For the adsorbent particles at the center of the fins, the only route of heat transfer to and from the adsorbent particles was through the fins. However, for the adsorbent particles at the edges of the fins, the adsorbate temperature also affected the adsorbent particles' temperature. For the adsorbent particles at the center of the fins, the temperature gradient was always higher during the desorption process than the adsorption process. The results also indicated that the effects of fin spacing on the temperature gradient inside the adsorber bed and the evaporator temperature were more significant under short cycle times (600 s) rather than long cycle times (1400 s). Comparing the temperature differences between the fins, and AAMR vs. fin spacing showed that 6 mm fin spacing was an optimum value for the finned tube adsorber bed packed with 2–4 mm silica gel beads.

REFERENCES

Alam, K.C.A., Saha, B.B., Kang, Y.T., 2000. Heat exchanger design effect on the system performance of silica gel adsorption refrigeration systems. Int. J. Heat Mass Transf. 43, 4419–4431.

Aristov, Y.I., Sapienza, A., Ovoshchnikov, D.S., Freni, A., Restuccia, G., 2012. Reallocation of adsorption and desorption times for optimisation of cooling cycles. Int. J. Refrigeration 35, 525–531.

Boelman, E.C., Saha, B.B., Kashiwagi, T., 1995. Experimental investigation of a silica gel-water adsorption refrigeration cycle- the influence of operating conditions on cooling output and COP. ASHRAE Trans. 101, 358–366.

Chua, H.T., Ng, K.C., Malek, A., Kashiwagi, T., Akisawa, A., Saha, B.B., 1999. Modeling the performance of two-bed, silica gel–water adsorption chillers. Int. J. Refrigeration 22, 194–204.

Demir, H., Mobedi, M., Ülkü, S., 2008. A review on adsorption heat pump: problems and solutions. Renew. Sustain. Energy Rev. 12, 2381–2403.

El-Sharkawy, I.I., Kuwahara, K., Saha, B.B., Koyama, S., Ng, K.C., 2006. Experimental investigation of activated carbon fibers/ethanol pairs for adsorption cooling system application. Appl. Therm. Eng. 26, 859–865.

Eun, T., Song, H., Hun, J., Lee, K., Kim, J., 2000. Enhancement of heat and mass transfer in silica-expanded graphite composite blocks for adsorption heat pumps: Part I. Characterization of the composite blocks. Int. J. Refrigeration 23, 64–73.

Eun, T., Song, H., Hun, J., Lee, K., Kim, J., 2000. Enhancement of heat and mass transfer in silica-expanded graphite composite blocks for adsorption heat pumps. Part II. Cooling system using the composite blocks. Int. J. Refrigeration 23, 74–81.

Farrington, R., Rugh, J., 2000. Impact of vehicle air-conditioning on fuel economy, tailpipe emissions, and electric vehicle range. In: Proceeding Earth Technol. Forum, Washington, D.C.

Freni, A., Tokarev, M.M., Restuccia, G., Okunev, A.G., Aristov, Y.I., 2002. Thermal conductivity of selective water sorbents under the working conditions of a sorption chiller. Appl. Therm. Eng. 22, 1631–1642.

Freni, A., Russo, F., Vasta, S., Tokarev, M., Aristov, Y.I., Restuccia, G., 2007. An advanced solid sorption chiller using SWS-1L. Appl. Therm. Eng. 27, 2200–2204.

Hendricks, T.J., 2001. Optimization of vehicle air conditioning systems using transient air conditioning performance analysis. In: SAE Conf. Proc. P.

Lambert, M.A., Jones, B.J., 2006. Automotive adsorption air conditioner powered by exhaust heat. Part 1: conceptual and embodiment Design. Proc. Inst. Mech. Eng. Part D J. Automob. Eng. 220, 959–972.

Lambert, M.A., Jones, B.J., 2006. Automotive adsorption air conditioner powered by exhaust heat. Part 2: detailed design and analysis. Proc. Inst. Mech. Eng. Part D J. Automob. Eng. 220, 973–989.

Lu, Y.Z., Wang, R.Z., Jianzhou, S., Zhang, M., Xu, Y., Wu, J., 2004. Performance of a diesel locomotive waste-heat-powered adsorption air conditioning system. Adsorption 10, 57–68.

Mahdavikhah, M., Niazmand, H., 2013. Effects of plate finned heat exchanger parameters on the adsorption chiller performance. Appl. Therm. Eng. 50, 939–949.

Pentchev, I., Paev, K., Seikova, I., 2002. Dynamics of non-isothermal adsorption in packed bed of biporous zeolites. Chem. Eng. J. 85, 245–257.

Poyelle, F., Guilleminot, J.J., Meunier, F., 1999. Experimental tests and predictive model of an adsorptive air conditioning unit. Ind. Eng. Chem. Res. 38, 298–309.

Saha, B.B., Chakraborty, A., Koyama, S., Aristov, Y.I., 2009. A new generation cooling device employing $CaCl_2$-in-silica gel–water system. Int. J. Heat Mass Transf. 52, 516–524.

Sapienza, A., Santamaria, S., Frazzica, A., Freni, A., 2011. Influence of the management strategy and operating conditions on the performance of an adsorption chiller. Energy 36, 5532–5538.

Sharafian, A., Bahrami, M., 2013. Adsorbate uptake and mass diffusivity of working pairs in adsorption cooling systems. Int. J. Heat Mass Transf. 59, 262–271.

Sharafian, A., Bahrami, M., 2014. Assessment of adsorber bed designs in waste-heat driven adsorption cooling systems for vehicle air conditioning and refrigeration. Renew. Sustain. Energy Rev. 30, 440–451.

Tamainot-Telto, Z., Critoph, R.E., 2001. Monolithic carbon for sorption refrigeration and heat pump applications. Appl. Therm. Eng. 21, 37–52.

Verde, M., Cortés, L., Corberán, J.M., Sapienza, A., Vasta, S., Restuccia, G., 2010. Modelling of an adsorption system driven by engine waste heat for truck cabin A/C. Performance estimation for a standard driving cycle. Appl. Therm. Eng. 30, 1511–1522.

Verde, M., Corberan, J.M., de Boer, R., Smeding, S., 2011. Modelling of a waste heat driven silica gel/water adsorption cooling system comparison with experimental results. In: ISHPC Conf., Padua, Italy, pp. 7–8.

White, J., 2012. CFD Simulation of Silica Gel and Water Adsorbent Beds Used in Adsorption Cooling System. University of Birmingham.

Wu, W., Zhang, H., Sun, D., 2009. Mathematical simulation and experimental study of a modified zeolite 13X–water adsorption refrigeration module. Appl. Therm. Eng. 29, 653–659.

Zhang, L.Z., Wang, L., 1997. Performance estimation of an adsorption cooling system for automobile waste heat recovery. Appl. Therm. Eng. 17, 1127–1139.

Zhang, L.Z., Wang, L., 1999. Effects of coupled heat and mass transfers in adsorbent on the performance of a waste heat adsorption cooling unit. Appl. Therm. Eng. 19, 195–215.

Zhang, L.Z., Wang, L., 1999. Momentum and heat transfer in the adsorbent of a waste-heat adsorption cooling system. Energy 24, 605–624.

Zhao, Y., Hu, E., Blazewicz, A., 2012. Dynamic modelling of an activated carbon–methanol adsorption refrigeration tube with considerations of interfacial convection and transient pressure process. Appl. Energy 95, 276–284.